Mercury Porosimetry Applied to Sono-Aerogels

L. ESQUIVIAS[*],[†] AND N. DE LA ROSA-FOX
*Dpto. Física de la Materia Condensada, Universidad de Cádiz, Campus Universitario del Río San Pedro,
Apdo.40, Puerto Real, 11517 Cádiz, Spain*
luis.esquivias@uca.es; esquivias@intas.be

Abstract. Sonogels are dense with fine and homogeneous structure because the absence of a common solvent of the metalorganic precursor + water and, mainly, because the ultrasound favour network reticulation. This fact represents that the elastic modulus is several order of magnitude higher than gels obtained without ultrasound. The combination of high stiffness and tiny porosity allows actual intrusion of Hg in a porosimetry experiment. In this paper the behaviour of under isostatic pressure a number of sonogels prepared under different conditions is presented.

Keywords: sonogel, aerogel, mercury intrusion, bulk modulus

1. Introduction

The interest on Hg porosimetry applied to gels comes about when it was considered that could be a tool to foreseen the behaviour during gel drying. However, it resulted that aerogels do not intrude Hg into the pores but the isostatic pressure induces gel compaction by pore collapse [1–3]. Woignier, Phalippou et al. [4] have studied extensively the behaviour of aerogels under isostatic pressure. They calculated the bulk moduli of aerogels and used the isostatic pressure for gel compaction. Pirard and Pirard have analysed theoretically the compression of light aerogels [5].

Sonogels are dense and their structure is fine and homogeneous, because of the absence of solvent for the sol obtaining and, mainly, by the initial cross-linked state of reticulation induced by ultrasound [6, 7]. This fact is reflected on their mechanical behaviour [8]. Other special characteristic of these gels is that ultrasounds promote hydrolysis resulting in a particulate structure. The standard pore size associated to this structure is ∼2–3 nm. According to this porosity, in a Hg intrusion porosimetry, the mercury could only

enter into the structure for pressures above 200 MPa. This pressure is hundred of times higher than the required for compaction of classic gels but in sono-aerogels actual intrusion occurs. The goal of this paper is to measure the stiffness increase of a set of sono-aerogels as a function of the heat-treatment, ultrasound dose and precursor used in the sol preparation.

2. Experimental

The sono-aerogels were elaborated by hydrolysis (pH [HCl] = 1.5) and polycondensation of tetramethoxysilane (TMOS). A device delivering to the system 0.6 w·cm^{-3} of ultrasound power was employed [7]. The total dissipated was 150 J·cm^{-3}. Sonogels, called STMxy, were prepared from TMOS ($R_w = 10$), heat-treated at y·100°C for 4 h after drying. Two sets of samples were prepared with this precursor. Series $x = M$ was prepared applying 150 J·cm^{-3} and series $x = H$, 300 J·cm^{-3}. Sonosols were poured in glass hermetic containers at 50°C until gelation. Hypercritical drying is performed in autoclave following the procedure already described in a previous paper [9].

The gels were texturally characterised by isothermal nitrogen adsorption in an automatic device. Horvath-Kawazoe method [10] has been employed

---

for adsorption branch to calculate the pore size distributions.

Mercury intrusion porosimetry was carried out on out-gassed monolithic sono-aerogels and then filling the container with Hg. The sample is pressurised to atmospheric pressure. We take as apparent density the value measured at this point. For the run, Hg pressure varied from 0.1 to 300 MPa and then depressurised. Runs with counterparts of aerogels placed into an impermeable membrane were also carried out with this double aim: to check the compression of the uncovered sample and to evaluate the actual volume intrusion. For this last purpose the data of the wrapped sample were taken as blank reference. The bulk density ρ_b is calculated from the irreversible shrinkage volume and intruded volume and from apparent density.

3. Results

The nitrogen adsorption isotherms are type IV of the IUPAC classification. This type features spherical and particulate agglomerations. Isotherms of STMH6 and STMM6 are practically identical. Both curves indicate that these aerogels have no macropores with a narrow distribution $\frac{dK}{dv} > 0$ of mesopores. The behaviour at low pressure indicates that some very fine porosity exits. The curve of the STMH9 sample corresponds to a pore distribution with shorter pore radius. The pores are interconnected. The plateau begins at a smaller relative pressure than the STMx6.

The pressurisation curves present a linear compression with increasing pressure then plastic deformation could take place and finally actual intrusion up to saturation. The depressurisation describes a hysteresis loop with mercury extrusion and partial recovering of the initial volume. After the run the samples presented both shrinkage and intruded mercury except for STMH6.

The STMM6 sample is compressed linearly 3-vol% up to approximately 35 MPa, for a higher pressure intrusion occurs (Fig. 1). The intrusion happened at two rates. The apparent density at 300 MPa is 1.40 g/cm^3 that represents that 73% of the initial pore volume is intruded. Depressurisation induces a partial mercury extrusion. For pressure lower than 100 MPa no extrusion is observed. An irreversible compaction of 0.18 cm^3/g is measured representing 12% volume reduction. In Fig. 2 are represented the pore volume distributions obtained from mercury intrusion and N2 adsorption-desorption isotherms.
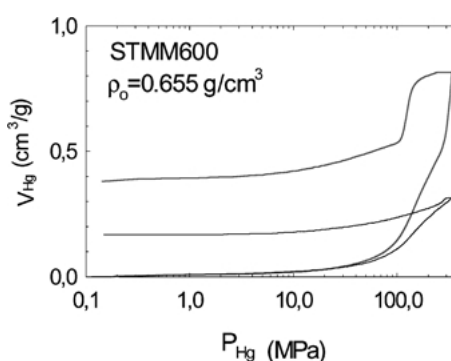

Figure 1. Pressurisation-depressurisation curves of the sample STMM6 free and encapsulated with a hermetic latex membrane.
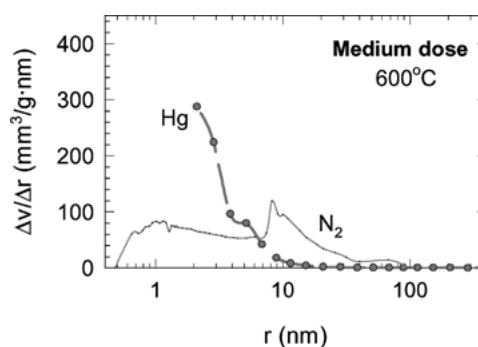

Figure 2. Pore size distribution from N$_2$ physisorption isotherm of the STMM6 before and after being compressed in the latex membrane. Dots correspond to the distribution obtained from mercury intrusion. Spline line is a guide for the eyes.

Applying the double of ultrasound dose than the above referred gel, intrusion begins, slightly, for pressure above 50 MPa and, abruptly, at 220 MPa. Extrusion occurs when the decreasing pressure is lower than 100 MPa. Below 70 MPa no extrusion is observed but just decompression. The ratio of irreversibly compacted volume is 6 vol%. The apparent density at the maximum of intrusion is 2.03 g/cm^3. There is 5 vol% of pore which is not filled by Hg. The pore volume distributions obtained by both methods are found in Fig. 3.

The porosimetry curves of the counterpart of this sample heat-treated at 900°C appear in Fig. 4. Intrusion begins for pressures as higher as 250 MPa for the maximum pressure remains free of mercury 85% of pore volume. Figure 5 are represented the pore volume distributions obtained from mercury intrusion and N$_2$ adsorption-desorption isotherms.
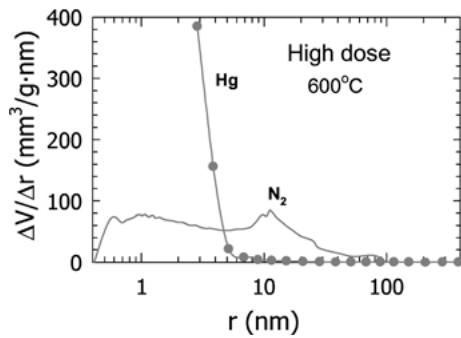
Figure 3. Pore size distribution from N_2 physisorption isotherm of the STMH6 sample before being compressed in the latex membrane. Dots correspond to the distribution obtained from mercury intrusion. Spline line is a guide for the eyes.

Figure 4. Pressurisation-depressurisation curves of the sample STMH9 free and encapsulated with a hermetic latex membrane.

Figure 5. Pore size distribution from N_2 physisorption isotherm of the same sample before being compressed in the latex membrane. Dots correspond to the distribution obtained from mercury intrusion. Spline line is a guide for the eyes.
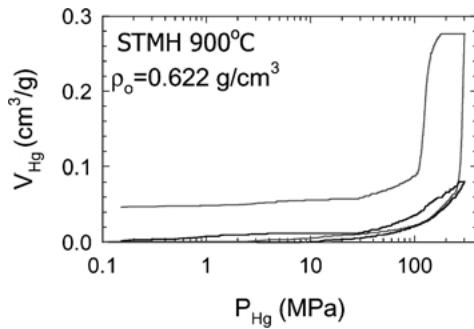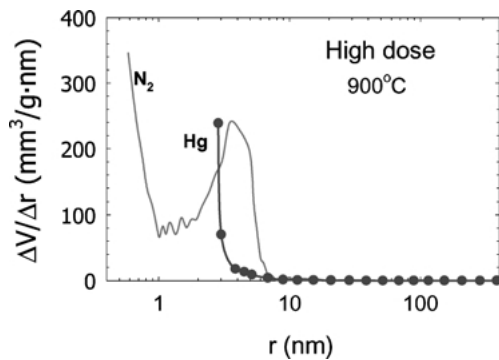
The STMM9 sample is intruded slightly at 40 MPa. Intrusion becomes sharp when the applied pressure attains 140 MPa. 3 vol% of pore volume is not intruded, according to the apparent density (2.07 g/cm^3) at 300 MPa.

Table 1. Bulk modulus, apparent density for $P = 0$, the threshold pressure for intrusion and the pore size that corresponds.

T (°C)		600	900	1100
STMH	K (MPa)	$2{,}12 \cdot 10^3$	$2.93 \cdot 10^3$	$2{,}79 \cdot 10^3$
	ρ_b (g · cm^{-3})	0.79	0.62	1.95
	P_u (MPa)/r_p	220/3	240/3	–
STMM	K (MPa)	$1{,}23 \cdot 10^3$	$1{,}56 \cdot 10^3$	$3{,}14 \cdot 10^3$
	ρ_b (g · cm^{-3})	0.66	0.75	2.21
	P_u (MPa)/r_p	80/9	130/6	–

In the bulk modulus of aerogels, K, has been evaluated as

$$K = -V\frac{dP}{dV} = \frac{1}{\rho_b}\frac{dP}{dv} \qquad (1)$$

from the linear part of the curve, where V is the sample volume, ρ_b the bulk density and v the sample specific volume reduction. The error is lower than 3% (Table 1).

4. Discussion

The intrusion in two steps in the sample STMM6 indicates a bimodal pore distribution. The apparent density at 300 MPa (1.40 g/cm^3) indicates that 23% of the pore volume, corresponding to pore of radius smaller than 2 nm, are not intruded. The total volume shrinkage is 30% of the encapsulated sample initial volume that represents 10% of length contraction. As can be see in Fig. 2 by comparison with the data obtained from N_2 physisorption, this diminution corresponds mainly to the reduction of pore larger than 8 nm radius. The main difference lies on 1–10 nm range where the compressed sample increases the number of pore, as it can be seen in Fig. 2–10 nm range where the compressed sample increases the number of pore.

The more noticeable feature of pressurisation/depressurisation curve of the STMH6 sample is that extrusion is complete in spite that 81% of intrude volume corresponds to pores smaller than 10 nm. The bulk modulus (Table 1) is double than that of the sample STMM6, in which 76% of mercury is intrude in pore smaller than 10 nm. The total volume shrinkage is the same than the former one. By comparison with the data obtained from N_2 physisorption (Fig. 3), this diminution corresponds mainly to the reduction of pores larger than 5 nm radius. Differently than before, the compressed sample increases the number of pore 2–5 nm range. No bimodality is observed.

The STMM9 and STMH9 lose 7% and 10%, respectively, i.e., 2% and 3% in length. In the STMH9 sample, which is less dense than expected, only 24% of the total porous volume is occupied by mercury, indicating the presence close porosity. The pore volume distribution (Fig. 5) obtained by Hg intrusion is shifted 2 nm downward the scale respect to that obtained by N_2 physisorption.

As a consequence of this diminution of pore volume, the density increases with pressure and, hence, the bulk modulus increases.

When $\frac{dP}{dv} = A(v)$

$$\frac{dK}{dv} = \frac{1}{\rho_b} \frac{dA}{dv} - \frac{A}{\rho_b^2} \frac{d\rho_b}{dv} \qquad (2)$$

there are two concurrent terms to the variation of K: the change of the $P(v)$ slope is balanced with an increase of density, whether apparent, if caused by intrusion, or real if it is by compaction.

When the sample compacts, $\frac{dK}{dv} > 0$, since $\frac{dv}{dP} > 0$, and consequently $\frac{\Delta \rho}{\rho_o} < \frac{\Delta A}{A_o}$.

Thus, K increases when the relative density increase is lesser than the relative increase of the $P(v)$ slope.

If ρ_o and ρ_b are the bulk density at the pressure P_o and P, respectively, then:

$$A(v) > A_o \frac{\rho_b}{\rho_o} = \frac{A_o}{(1 - \rho_o v)} \qquad (3)$$

At the same time, $\rho_o v > 0$, it follows that $A(v)$ increases monotonically.

This means that if there is an important density increase (i.e., apparent specific volume decrease), it could be only due to intrusion.

Integrating (5), with $P = P_0$, $v = v_o = 0$ and taking, $\frac{A_o}{\rho_o} = K_o$ in the terms of ref. [2], the result is:

$$\frac{V_{Hg}}{V} = \frac{V_o - V}{V} < 1 - \exp\left(-\frac{\Delta P}{K_o}\right) \qquad (4)$$

$\rho_o v = V_{Hg}/V_o$ is the mercury volume (whether intruded or occupying the part of the initial volume of the sample) relative to the initial sample volume. V is sample apparent volume at the pressure P. Also:

$$P > P_o - K_o \ln\left(\frac{V}{V_o}\right) \qquad (5)$$

When $K_o \gg \Delta P$, which always happens in our gels,

(5) can be approximated as:

$$\Delta P > \frac{V_{Hg}}{V_o} K_o \qquad (6)$$

This is the condition for being in plastic regime. Consequently, in this situation, when $dP/dv \approx$ constant, according to (4), and (6) and:

$$\Delta K \cong \Delta P \qquad (7)$$

In the plastic regime, the modulus changes with the volume according to a power law [2]

$$K = K_o \left(\frac{V_o}{V}\right)^m \qquad (8)$$

Our conditions (5) and (6) require $m > 1$. In the same way, from ref. [2]

$$A = A_o \left(\frac{V_o}{V}\right)^{m+1} \qquad (9)$$

that combined with (3) gives $\left(\frac{\rho_b}{\rho_o}\right)^m > 1$ ($m > 0$ since always $\rho_b > \rho_o$). Accordingly (8), if $m < 0$, the bulk modulus decreases and $\Delta P(V_{Hg})$ does not stand for condition (4), i.e., there is intrusion. The experimental curve $P(V_{Hg})$ is going far above the straight line $\Delta P = \frac{V_{Hg}}{V_o} K_o$.

Figures 6 and 7 account, respectively, for one case where there is intrusion at relative low pressure (STMH6) and other case in which intrusion occurs at high-pressures (STMH9). Both cases stand for our
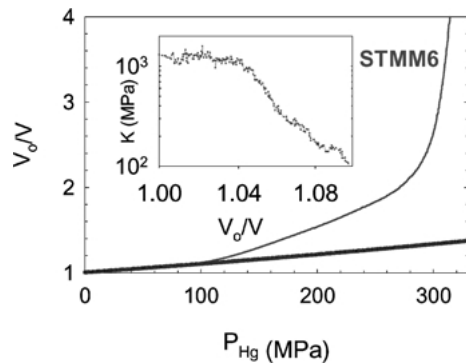

Figure 6. Representation showing a pressurisation curve (STMM6) sample above the "border line" between intrusion/compaction. In this case the experimental data indicate that there is intrusion. Inset: Representation of K as a function of the apparent sample volume. Intrusion starts for $P_{Hg} \sim 100$ MPa.
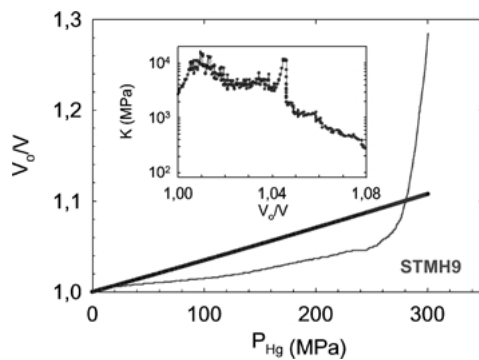
Figure 7. Representation showing a pressurisation curve that goes below the "border line" between intrusion/compaction meaning that there is no intrusion but compaction up to $P = 230$ MPa. The inset is a representation of K as a function of the apparent sample volume. Intrusion starts for $V_{o}/V \sim 1.05$.

condition. In the first case, above $V_{o}/V \cong 1.05$, K decreases, meaning that intrusion began at this point. K slightly increases in the range where there is compaction (inset in Fig. 7). In the second case the experimental data are below that border meaning that there is no intrusion but compaction up to $P = 230$ MPa. Important increases of K is seen up to $V_{o}/V \sim 1.02$ ($P_{Hg} = 80$ MPa) where K becomes several time higher than K_{o}. Then it decreases, probably destroying a part of the pore structure. A huge increase is produced for $V_{o}/V \sim 1.04$ ($P_{Hg} = 260$ MPa), just before the threshold for intrusion meaning that intrusion began.

5. Conclusions

1. The pressurisation curves of sono-aerogels behave unusually and actual intrusion occurs. The depres-surisation describes a hysteresis loop with extrusion of the intruded mercury and partial recovering of the initial volume.
2. Mercury porosimetry is an adequate probe for sono-aerogels, giving true information of the sonogel structure, at least on the gel under isostatic pressing.
3. Compression reduces the pore size, increasing the number of them in the 1–10 nm range.
4. Intrusion occurs when a finite increase of pressure follows power law $\Delta P = \frac{V_{Hg}}{V_{o}} K_{o}$ or the bulk modulus $K = K_{o}(\frac{V_{o}}{V})^{m}$ with $m < 0$.

Acknowledgment

References

1. R. Pirard, S. Blacher, F. Brouers, and J.P. Pirard, J. Mater. Res. **10**(8), 2114 (1995).
2. G. Scherer D.M. Smith, and J. Anderson, J. Non-Cryst. Solids **186**, 316 (1995).
3. R. Pirard, B. Heinrichs, O.Van Cantfort, and J.B. Pirard, J. Sol-Gel Science & Technol. **13**, 335 (1998).
4. L. Duffours, T Woignier, and J. Phalippou, J. Non. Cryst. Solids **194**, 283 (1996).
5. R. Pirard and J.P. Pirard, J. Non. Cryst. Solids. **212**, 262 (1997).
6. J. Zarzycki, Heterogeneous Chemistry Reviews **1**, 243 (1994).
7. L. Blanco, R. Esquivias, M. Litrán, M. Piñero, M. Ramírez-del-Solar, and N. de la Rosa-Fox, Applied Organometallic Chemistry **13**, 399 (1999).
8. J. Zarzycki, J. Non. Cryst. Solids **100**, 359 (1988).
9. L. Esquivias, J. Rodríguez-Ortega, C. Barrera-Solano, and N. de la Rosa-Fox, J. Non-Cryst-Solids **225**(1–3) 239 (1998).
10. G. Horvath and K. Kawazoe, J. Chem. Eng. of Japan **16**(6), 470 (1983).